

# Blends of Poly(ethylene terephthalate) with Co[poly(ethylene terephthalate-*p*-oxybenzoate)]. IV. Interchange Reactions and Their Effects on the Thermal and Crystallization Behaviors

CHENG-FANG OU<sup>1</sup> and CHEN-CHONG LIN<sup>2,\*</sup>

<sup>1</sup>National Chin-yi Institute Technology, Department of Chemical Engineering, Taichung, Taiwan, Republic of China;

<sup>2</sup>National Chiao Tung University, Institute of Materials Science and Engineering, Hsinchu, Taiwan, Republic of China

## SYNOPSIS

Poly(ethylene terephthalate) (PET) was blended with a co[poly(ethylene terephthalate-*p*-oxybenzoate)] (POB-PET) copolyester which is a liquid crystalline polymer consisting of *p*-oxybenzoate and ethylene terephthalate units in a 40/60 mol ratio (P46). The level of P46 liquid crystalline polymer varies from 10 to 50 wt %. All the blends were prepared by melt-mixing in a Brabender Plasticorder at 275°C for different times. The thermal and crystallization behaviors of blends depend on the blending time and the composition of blends, viz., the content of the *p*-oxybenzoate (POB) moiety incorporated into the blends. The interchange reactions detected by proton NMR analysis occur during the processing at a greater level if the blending time increases. These interchange reactions hinder the crystallization processes of PET and result in a decrease of the melting point, the heat of fusion, crystallization temperature, and the heat of crystallization of the original PET. The effects of the interchange reaction on thermal and crystallization behaviors of the blends may be attributed to the insertion of the rigid POB units into the soft PET chain. © 1996 John Wiley & Sons, Inc.

## INTRODUCTION

Poly(ethylene terephthalate) (PET) is one of the engineering plastics that has been studied as a component of many polymer blends. PET crystallization can be increased by the addition of polymeric nucleating agents such as linear low-density polyethylene (LLDPE),<sup>1</sup> poly(methyl methacrylate) (PMMA),<sup>2</sup> poly(phenylene sulfide) (PPS),<sup>3</sup> high-density polyethylene (HDPE),<sup>3</sup> and liquid crystalline polymer (LCP).<sup>4-9</sup> The alloying of PET with PMMA was reported to accelerate the crystallization significantly and was most pronounced in a 85/15 PET/PMMA blend.<sup>2</sup> Other PET/LCP blends of PET/VLC (trade name Vectra A900) and PET/KLC (PHB/PET = 80/20 mol ratio) were studied by Misra et al.<sup>7</sup> According to these investigations, VLC

and KLC act like nucleating agents for PET crystallization and this effect probably reaches a maximum at an LCP level between 0 to 5 wt %. In the range from 10 to 15 wt %, VLC and KLC possibly destroy the symmetry of PET, thus resulting in decreases in  $\Delta H_f$ ,  $\Delta H_c$ , and  $T_m$ . From these earlier results, it is seen that the crystallization behavior of PET blends is influenced by the composition and amount of the second component, chemical compatibility, and the degree of dispersion achieved in the mixing process.

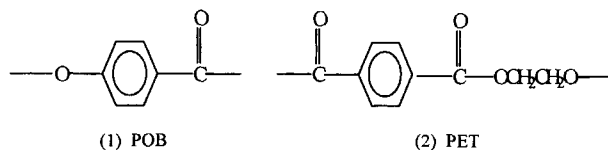
The transesterification or ester exchange reaction in the polyester blends can play an important role in their miscibility and consequent properties. This reaction has been found to take place in many PET blends such as PET/PBT,<sup>10</sup> PET/PC,<sup>11,12</sup> and PET/polyacrylate (PA),<sup>13-17</sup> as well as in the blends with *p*-oxybenzoate (POB)-PET copolyester such as PBT/POB-PET<sup>18</sup> and PC/POB-PET.<sup>19,20</sup> It is well known that the transreaction in the polymer blends

\* To whom correspondence should be addressed.

depends strongly on their initial compatibility and blending condition. This includes temperature, duration of mixing, preparation method, viscosity match, and presence of catalysts<sup>21</sup> as well as inhibitors.<sup>22-24</sup> In the previous investigations of the PET blends with the POB-PET copolyester,<sup>4-9</sup> several conclusions concerning the miscibility in these blends exists, and no specific interchange reaction between the components has been shown.

The objective of this present investigation was to examine PET with POB-PET copolyester for the existence of possible interchange reaction between the components, the relation of the level of interchange reaction as a function of blending time, and the effect of the level of interchange reaction on the thermal and crystallization behaviors of PET in a blend by differential scanning calorimetry (DSC) and proton nuclear magnetic resonance (NMR) analyses.

The chemical structure of the co[poly(ethylene terephthalate-*p*-oxybenzoate)] (POB-PET) copolyester consists of the following two moieties:



## EXPERIMENTAL

### Materials

Co[poly(ethylene terephthalate-*p*-oxybenzoate)] copolyester of P46 was synthesized according to the procedure reported in our previous article.<sup>25</sup> The PET resin was kindly supplied by Far East Textile Co (Taiwan) having an intrinsic viscosity (IV) of 0.62 (dL/g) in 60/40 (w/w) phenol/tetrachloroethane at 30°C.

### Blending Method

PET and P64 copolyesters were dried *in vacuo* at 105°C for 48 h before blending to avoid a degradation reaction caused by moisture. The weight ratios of PET to copolyester in the system tested were 90/10, 85/15, 70/30, and 50/50. The blends were prepared by melt-mixing in a Brabender Plasticorder at 275°C and at a mixing blade speed of 30 rpm. Samples were taken at various times from the mixing bowl and immediately quenched in liquid nitrogen.

### DSC Measurement

DSC was used to characterize the thermal and crystallization behaviors of the blended samples. The size of samples was reduced to about 0.5 mm in diameter by a cutting mill. The weight of all samples was kept between 10 and 11 mg for DSC evaluation. DSC measurements were carried out in a DuPont DSC cell equipped with a DuPont 2000 thermal analyst system. Samples were heated to 305°C at a heating rate of 10°C/min under a nitrogen atmosphere, held for 5 min to destroy anisotropy, and then cooled at 10°C/min to 30°C. Both thermal and crystallization parameters were obtained from the heating and cooling scans.

### NMR Spectra

For the NMR spectra, a 5–10 wt % solution of the blend in deuteriated trifluoroacetic acid (TFA) was prepared. The spectra were then taken within several hours of the sample dissolution and with tetramethylsilane (TMS) as the internal standard. The spectra were obtained by a Varian Model Unity-300 NMR spectrometer operating at 300 MHz for observing protons.

## RESULTS AND DISCUSSION

### Identification of Interchange Reaction by NMR Analysis

The occurrence of increasing levels of interchange reaction in the PET/P46 blends after blending times of 3, 8, 20, 40, and 80 min in PET/P46 weight ratios of 85/15, 70/30, and 50/50 was tested. The extent of the interchange reaction depends also on the time-temperature history of the blend. Figure 1 illustrates the 300 MHz proton NMR spectrum for P46 in trifluoroacetic acid solution and shows the assignments for the resonances. The sharp signals at 8.2 and 4.9 ppm correspond to the proton of the terephthalate and the methylene proton, respectively. According to Lenz<sup>26</sup> and Nicely et al.,<sup>27</sup> the peak at higher magnetic field (7.5 ppm) corresponds to the POB-POB dyad while the other (7.4 ppm) is due to the POB-PET dyad. Spectra of these types have been measured to determine the fraction of the POB repeat units that are bonded to a PET unit or to another POB unit. Figure 2 shows the POB-PET and POB-POB dyads region of the NMR spectra of the PET/P46 (70/30) blend after different blending times. It can be seen that the ratio of POB-PET to POB-

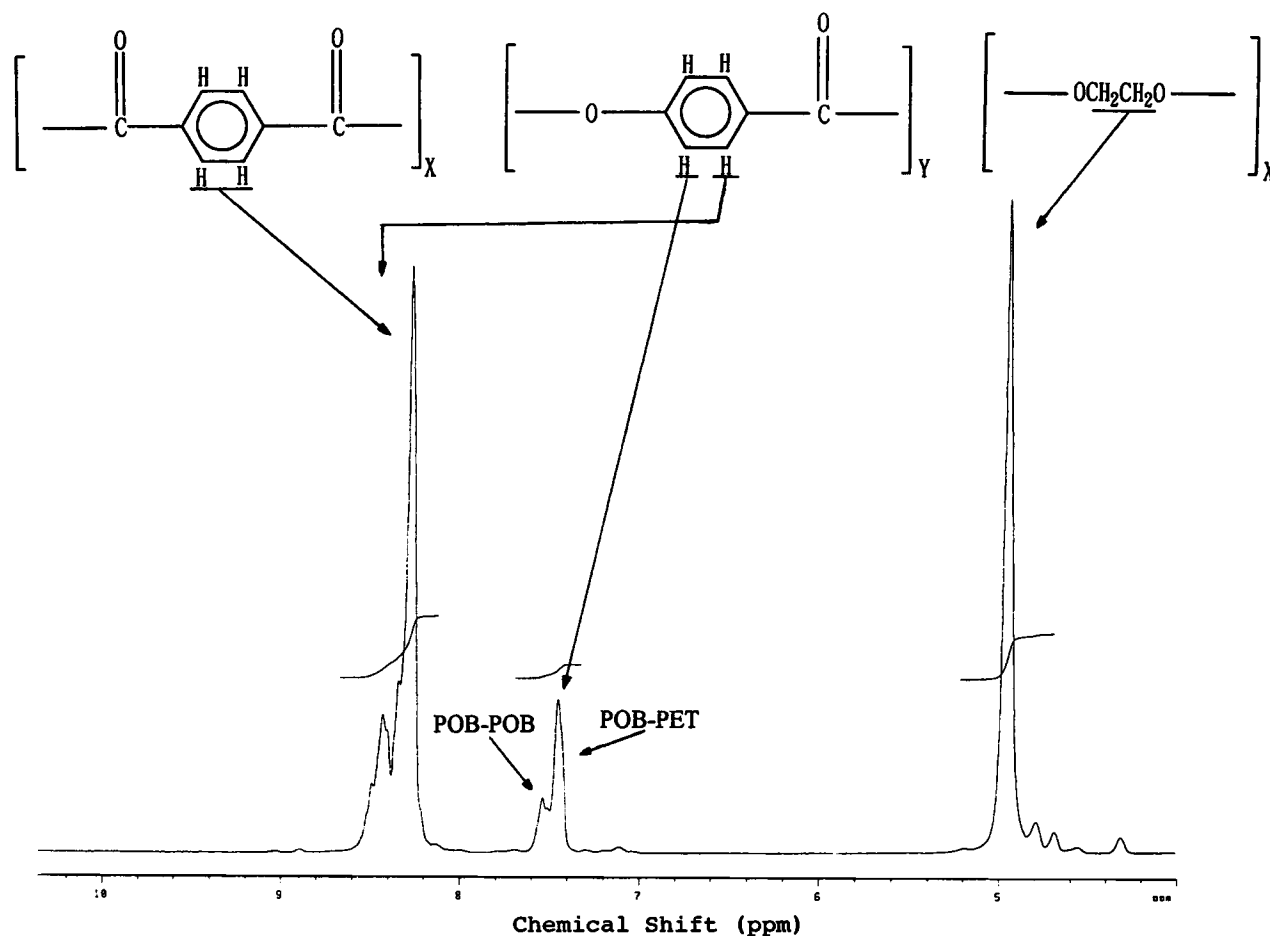


**Figure 1** Proton NMR spectrum at 300 MHz with the assignments of the absorptions for P46 dissolved in trifluoroacetic acid.

POB dyads increases progressively with blending time. This result proves that a greater level of interchange reaction can be obtained at a longer blending time. Figure 3 shows the mol % of POB bonded to PET unit as a function of blending time for PET/P46 (85/15), PET/P46 (70/30), and PET/P46 (50/50) compositions. It is seen clearly that the mol % of POB bonded to the PET unit increases with blending time for these blends. These results reveal that the interchange reaction already occurs within 3 min blending and the level of the interchange reaction increases with the blending time in these blends. The different slopes of the line at the periods between 0 and 3 min and between 3 and 80 min representing the rates of interchange reaction depend on the PET/P46 ratio. These results seem to indicate that the level of the interchange reaction depends strongly on both the composition of the blend and duration of mixing.

### Thermal and Crystallization Behavior in PET/P46 Blends

The results of DSC heating and cooling scans for PET and PET/P46 blends after 8 min blending at 275°C are shown in Figure 4(a) and (b), respectively. It is evident that there is a distinct glass transition temperature ( $T_g$ ), an exothermic recrystallization peak, and an endothermic melting peak in all of the heating scans, with the exception of the 50/50 PET/P46 blend for which the recrystallization peak disappears. The recrystallization exotherm is due to the rapid cooling of the melt in liquid nitrogen, making the full crystallization of PET difficult. The disappearance of the recrystallization peak in the 50/50 blend indicates a fully hindered recrystallization of PET and the total crystallinity ( $\Delta H_f$ ) of the blend is due to the primary crystallization at the rapid cooling process conditions. On the other hand, there is a distinct exothermic crystallization peak

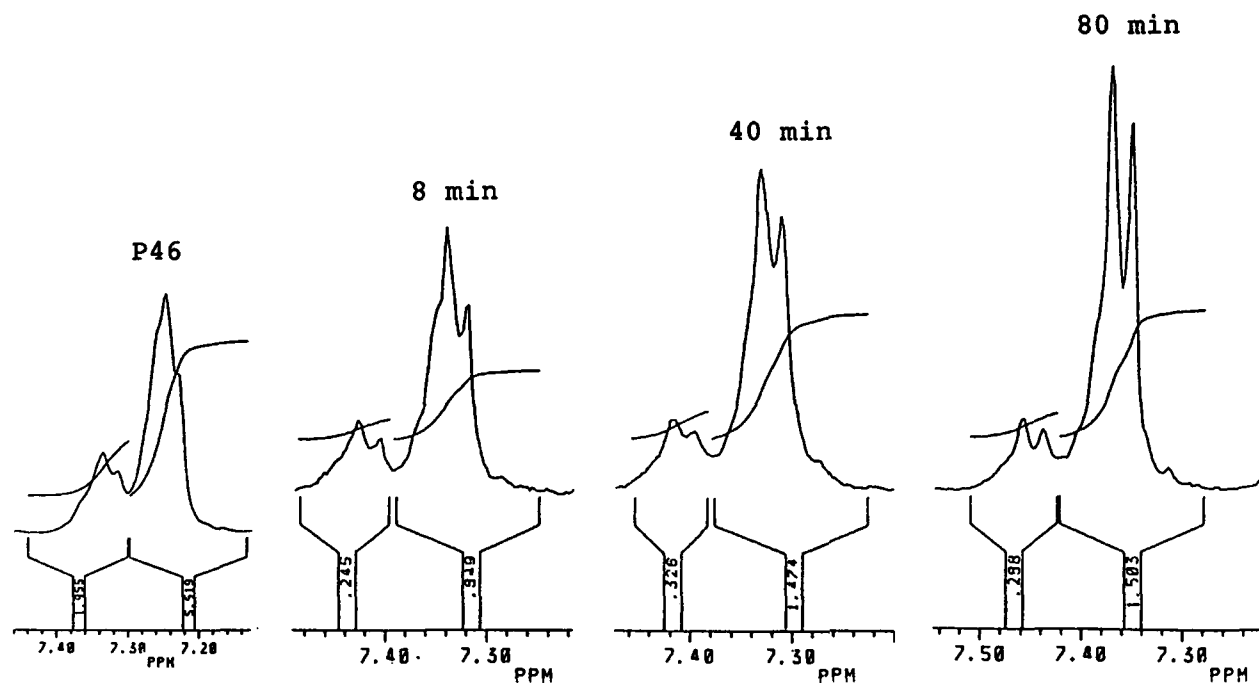


Figure 2  $^1\text{H-NMR}$  spectra of PET/P46 (70/30) blends after different blending times.

in all the cooling scans. The various thermal and crystallization parameters determined from heating and cooling scans of the blends are given in Table I. It is obvious that all the onset temperatures of recrystallization and recrystallization temperatures ( $T_{rc}$ ) measured at the peak of recrystallization exotherm for the blends, are lower than those of pure PET. The onset temperatures of recrystallization of

the blends decrease with increasing P46 content. The  $T_{rc}$  goes through a minimum at ca. 30% P46 as a function of P46 concentration. These results would appear to reveal that the recrystallization mechanism of PET in blends might be different from that of pure PET.

The onset temperature of melting and melting peak width ( $\Delta T_m$ ) are related to lesser stability and the distribution of the crystallites, respectively. A clear decrease of the onset temperature of melting and  $T_m$  is found in the blends with respect to those of pure PET. Moreover, the higher the content of P46 in the blends, the greater is this decrease. The  $\Delta T_m$  increases from that of pure PET with increasing P46 content. The value of  $\Delta T_m$  for 90/10 PET/P46 blend is  $2^\circ\text{C}$  higher than that of pure PET (i.e.,  $47^\circ\text{C}$ ). As the P46 content increases over the range from 10 to 50%, the value of  $\Delta T_m$  increases a further  $13^\circ\text{C}$ . These results indicate that the crystals generated in such blends are less perfect than those found in pure PET and that they continue losing perfection as the P46 content increases.

The composition dependence of the crystallization parameters during cooling of the PET/P46 blends are given in Table I. The crystallization peak temperature ( $T_c$ ) and crystallization widths ( $\Delta T_c$ ) for the 90/10 PET/P46 blend are higher and narrower than those of pure PET, respectively. On the other hand, the heat of crystallization ( $\Delta H_c$ ) for the 90/10 PET/P46 blend is higher than that of pure

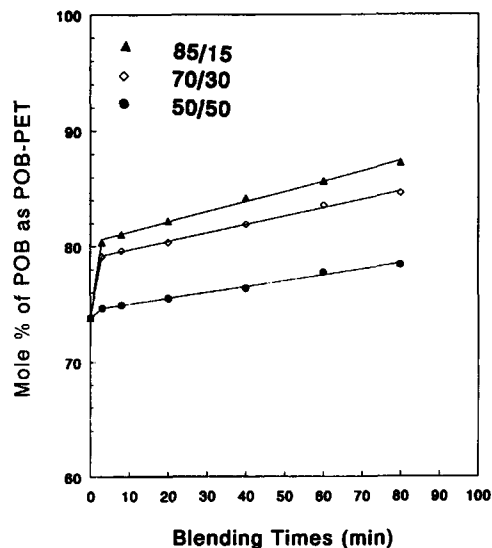
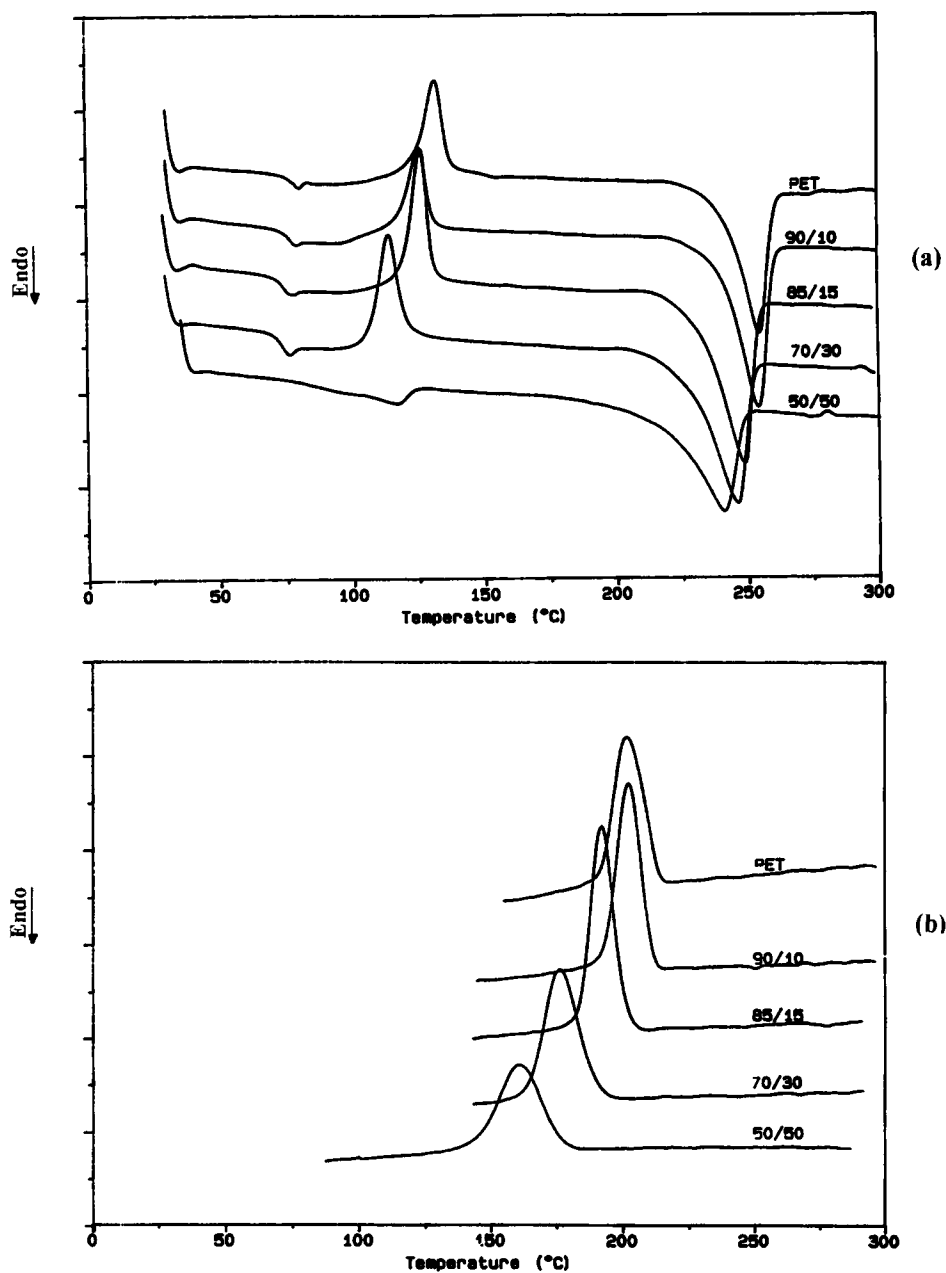


Figure 3 Mol % of POB connected to PET (i.e., POB-PET Dyad) after different blending times in the 85/15, 70/30, and 50/50 PET/P46 blends.



**Figure 4** (a) DSC thermograms of PET/P46 blends with different wt % of P46 after 8 min blending (heating scans). (b) DSC thermograms of PET/P46 blends with different wt % of P46 after 8 min blending (cooling scans).

PET (39.9 J/g). If the crystallization rate were defined as the heat of crystallization in a unit of time ( $\Delta H_c/\text{time}$ ), the crystallization rate of the 90/10 PET/P46 blend is higher than that of pure PET (0.180 J/g s). Thus, the crystallization of PET in the 90/10 blend exhibits a significant acceleration. On the contrary, when the P46 content is higher than 15%, the onset temperature of crystallization,  $T_c$ ,  $\Delta H_c$ , and crystallization rate all decrease with

increasing P46 content. These results seem to reveal that the blends with lower P46 content (<10%) accelerate the crystallization of pure PET, but the blends with higher content (>15%) inversely hinder the crystallization of pure PET. The crystallization results of PET/P46 blends are in agreement with an earlier crystallization study<sup>7</sup> which showed that PET crystallization from the melt was accelerated by blending with only a small quantity of a liquid

**Table I** DSC Data of PET/P46 Blends After 8 Min Blending

From Heating Scans										
(PET/P46) Composition	Recrystallization					Melting				Difference
	$T_g$ (°C)	Onset (°C)	$T_{rc}$ (°C)	$\Delta T_{rc}$ (°C)	$\Delta H_{rc}$ (J/G)	Onset (°C)	$T_m$ (°C)	$\Delta T_m$ (°C)	$\Delta H_f$ (J/g)	$\Delta H_f - \Delta H_{rc}$ (J/g)
100/0	73	116	133	34	26.9	220	253	47	39.7	12.8
90/10	74	110	127	33	16.8	219	253	49	43.3	26.5
85/15	73	108	127	34	20.1	211	249	50	47.3	27.2
70/30	72	99	115	43	19.0	203	246	53	46.0	27.0
50/50	83	—	—	—	—	192	241	62	40.1	40.1

From Cooling Scans						
(PET/P46) Composition	Crystallization					
	Onset (°C)	$T_c$ (°C)	$\Delta T_c$ (°C)	$\Delta H_c$ (J/g)	$\Delta H_c$ /Time (J/g s)	
100/0	216	200	37	39.9	0.180	
90/10	216	202	32	42.0	0.219	
85/15	210	193	36	42.2	0.195	
70/30	199	177	46	40.3	0.146	
50/50	184	161	54	33.1	0.102	

crystalline polymer (LCP) (within 20%) which might act as a nucleating agent.

### Interchange Reaction Effect

In general, where units of the same chemical structure in two distinct polymers cocrystallize, adjacent and dissimilar units of polymer components in the polyblends can act as impurities and deform the crystal structure.<sup>26</sup> Thus, depressions of the values of  $T_m$  and  $\Delta H_f$  with blend composition are often observed. For instance, the retardation of PET crystallization and lowering of its degree of crystallinity and crystallization rate in miscible blends of PET/PAr have been reported.<sup>13-17</sup> The decrease in the crystallinity of these blends was attributed to the inclusion of the rigid PAr unit in PET chains which causes a decrease in their crystallizable segment length.

To investigate the effect of the interchange reaction formed in the PET/P46 melt on thermal and crystallization behaviors, mixtures of the components in a 50/50 weight ratio were blended for 8, 20, 40, 60, and 80 min at 275°C. Figure 5(a) and (b) show the DSC heating and cooling scans for the 50/50 PET/P46 blends after different blending times, respectively. The thermogram obtained for pure

PET at 8 min blending time is also shown. Different thermal behavior is observed for the pure PET and the blends. PET shows a distinct glass transition with a  $T_g$  value of 73°C and, after that, an exothermic recrystallization peak (133°C) and an endothermic melting peak (253°C). The values of  $T_g$  for the blends are always higher than that of pure PET. The reasons for the jump in the glass transition temperature may be explained on the basis of the incorporation of rigid POB segment into the PET chains due to the interchange reaction during blending.

For all the blends, no recrystallization peak appears, indicating that PET is already unable to crystallize during the heating scan even after only 8 min blending. The total crystallinity ( $\Delta H_f$ ) of the blend is contributed by the primary crystallization during the rapid cooling process. With respect to the melting behavior, changes with blending time in the values of  $T_m$  and  $\Delta H_f$  are shown in Figure 6. The points at 0 min blending time correspond to pure PET. The values of  $T_m$  for blends exhibited a progressive decrease with blending time, indicating that the PET crystallites are less perfect in the blends and that they continue losing perfection as the blending time increases. The values of  $\Delta H_f$  increase slightly to 8 min but decrease with increasing

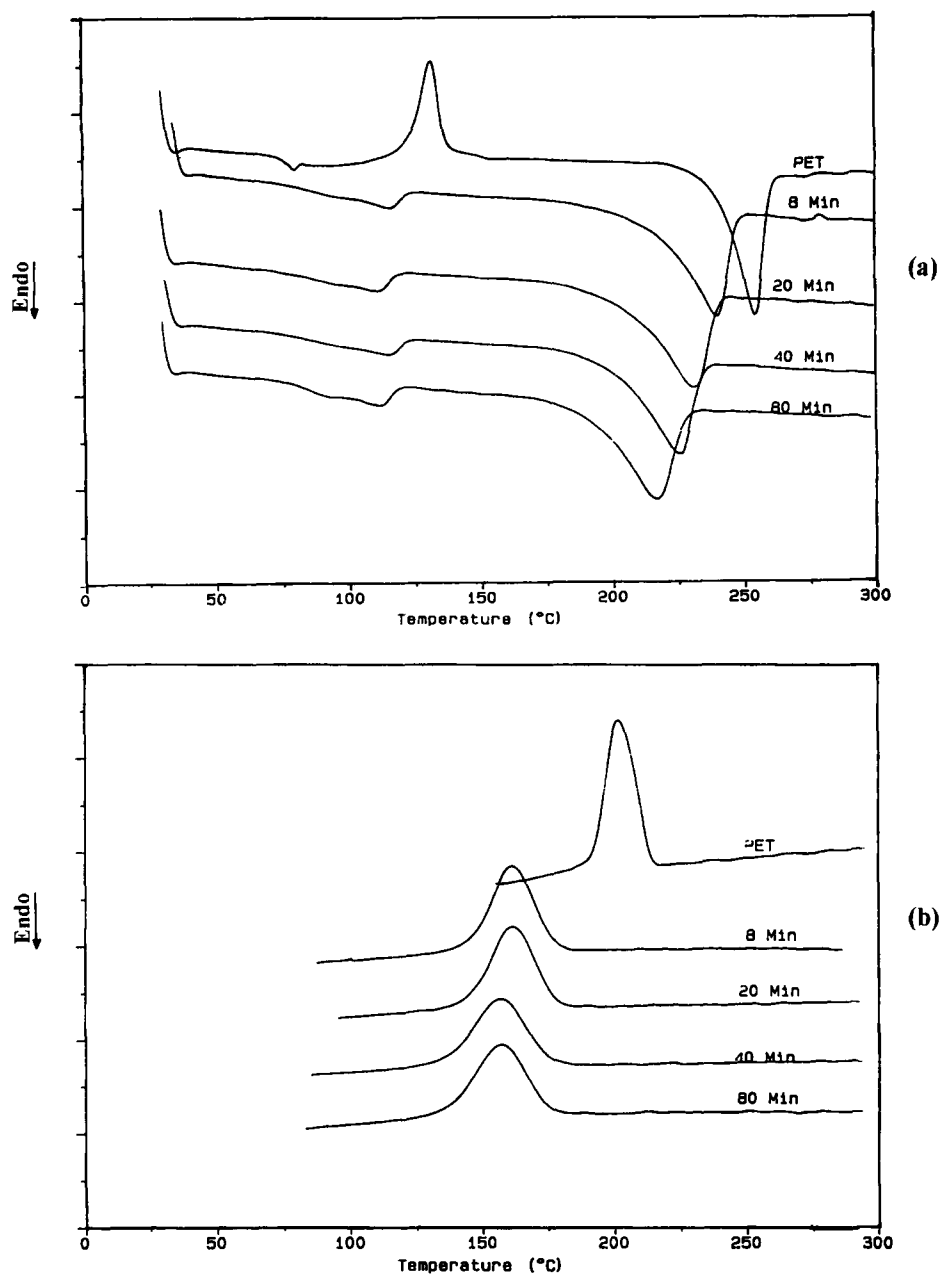


**Figure 5** (a) DSC thermograms of PET/P46 (50/50) blends after different blending times (heating scans). (b) DSC thermograms of PET/P46 (50/50) blends after different blending times (cooling scans).

blending time after 8 min. The depression of  $\Delta H_f$  indicates that progressively hindered crystallization of PET is evident with increasing blending time.

The crystallization parameters of crystallization onset temperature and  $T_c$  obtained from the cooling scans are shown in Figure 7. The crystallization onset temperatures of the blends are in the vicinity of 183°C and much lower than that of pure PET (216°C). A shift in the crystallization onset tem-

perature represents modification of the nucleation process. The crystallization peak temperature ( $T_c$ ) represents the temperature at the maximum crystallization rate. The  $T_c$  of the 50/50 PET/P46 blend after 8 min blending is at 161°C which is 39°C lower than that of pure PET (200°C). As the blending time increases from 8 to 80 min, the  $T_c$  decreases further in the order of 5°C. Changes in the crystallization peak width ( $\Delta T_c$ ) and the heat of crystalli-

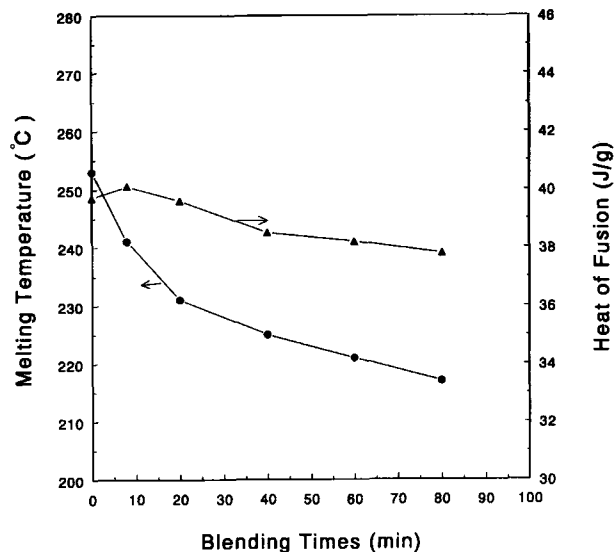


**Figure 6** Melting temperatures and heat of fusion of PET/P46 (50/50) blends after different blending times. The points at 0 min blending time correspond to pure PET.

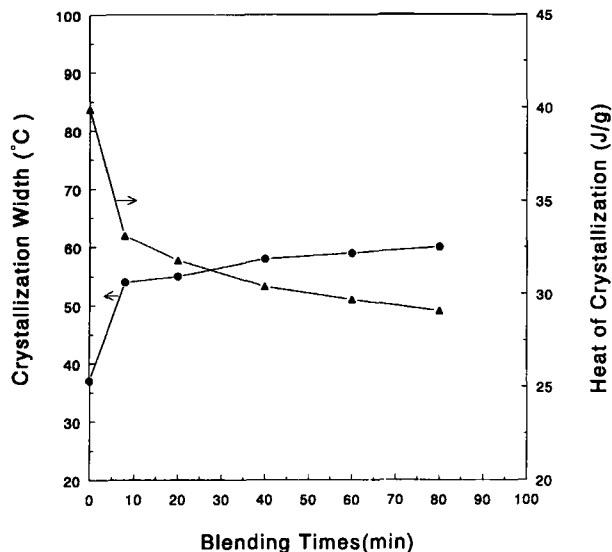


**Figure 8** Crystallization peak width and heat of crystallization in PET/P46 (50/50) blends after different blending times. The points at 0 min blending time correspond to pure PET.

zation ( $\Delta H_c$ ) are related to the overall crystallization rate and the extent of crystallization, respectively. The values of  $\Delta T_c$  and  $\Delta H_c$  of the blends obtained from the cooling scans are shown in Figure 8. As can be seen in Figure 8, all the crystallization peak widths for the blends are broader, compared to pure PET, and increase with increasing blending time. Furthermore, the values of  $\Delta H_c$  for the blends are

smaller than that of PET and decrease with increasing blending time. The broader crystallization exotherm in the blend is attributed to hindered crystallization of PET. This effect is also supported by the fact that both  $T_c$  and the values of  $\Delta H_c$  of the blends are always lower than those of pure PET. The crystallization rate decreases with increasing blending time as shown in Figure 9. These results may be attributed to a hindered crystallization, due

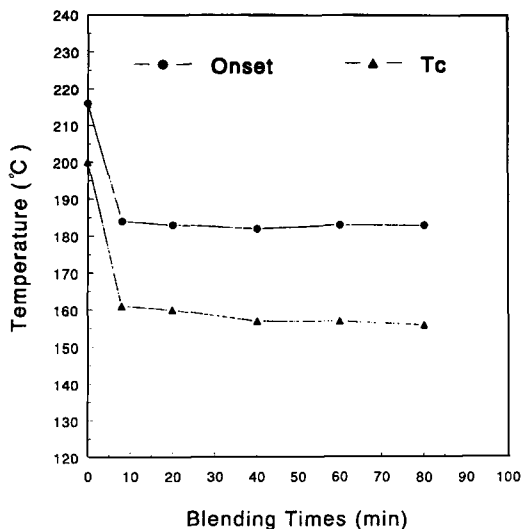


**Figure 7** Onset temperature of crystallization and crystallization temperatures in PET/P46 (50/50) blends after different blending times. The points at 0 min blending time correspond to pure PET.

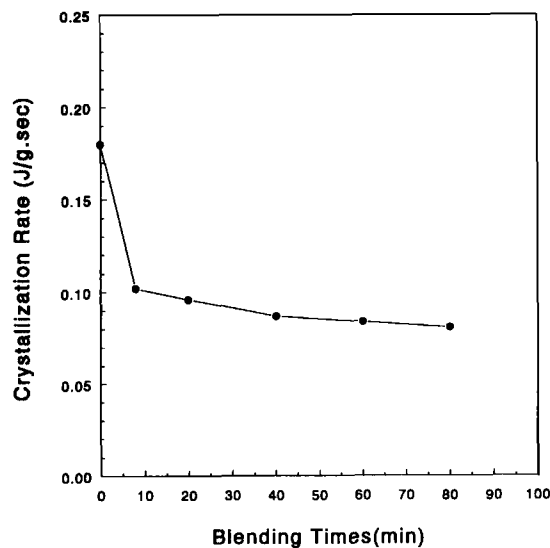


**Figure 9** Crystallization rate in PET/P46 (50/50) blends after different blending times. The points at 0 min blending time correspond to pure PET.



to the interchange reactions, and to the concomitant decrease in the crystallized segment length of PET. Thus, different levels of interchange reactions have been produced directly during melt-mixing. The change of nature of the material produced by the reactions leads to a progressive hindrance of PET crystallization.

## CONCLUSIONS

From NMR analysis, interchange reactions take place in the PET/P46 blends. The level of interchange reaction increases with increasing blending time. The interchange reaction would give rise to a hindrance of PET crystallization as detected by the DSC study. The greater the level of the interchange reaction, the more hindered is crystallization of the PET/P46 blends. The hindered crystallization of PET might be attributed to the insertion of the rigid POB units in PET chain and to the concomitant decrease in the crystallized segment length of PET.

## REFERENCES

1. L. Bourland, *Plast. Eng.*, **July**, 39 (1987).
2. V. M. Nadkarni and J. P. Jog, *Polym. Eng. Sci.*, **27**, 451 (1987).
3. V. M. Nadkarni, V. L. Shingankuli, and J. P. Jog, *J. Appl. Polym. Sci.*, **46**, 339 (1992).
4. E. G. Joseph, G. L. Wilkes, and D. G. Baird, *Prep. Am. Chem. Soc. Div. Polym. Chem.*, **24**, 304 (1983).
5. A. M. Sukhadia, D. Done, and D. G. Baird, *Polym. Eng. Sci.*, **30**(9), 519 (1990).
6. S. K. Battacharya, A. Tendokar, and A. Misra, *Mol. Cryst. Liq. Cryst.*, **153**, 501 (1987).
7. S. K. Sharma, A. Tendokar, and A. Misra, *Mol. Cryst. Liq. Cryst.*, **157**, 597 (1988).
8. C. F. Ou and C. C. Lin, *J. Appl. Polym. Sci.*, **54**, 1223 (1994).
9. C. F. Ou and C. C. Lin, *J. Appl. Polym. Sci.*, **56**, 1107 (1995).
10. R. S. Porter and L. H. Wang, *Polymer*, **33**, 2019 (1992).
11. F. Pilati, E. Marianucci, and C. Berti, *J. Appl. Polym. Sci.*, **30**, 1267 (1985).
12. P. Godard, J. M. Dekoninck, V. Dolcesaver, and J. Devaux, *J. Polym. Sci. Part A*, **24**, 3301 (1986).
13. M. Kimura, G. Salee, and R. S. Porter, *J. Appl. Polym. Sci.*, **29**, 1629 (1984).
14. J. I. Eguiazabal, M. E. Calahorra, M. M. Cortazar, and J. J. Iruin, *J. Polym. Eng. Sci.*, **24**, 608 (1984).
15. J. I. Eguiazabal, G. Ucar, M. Cortazar, and J. J. Iruin, *Polymer*, **27**, 2013 (1986).
16. J. I. Eguiazabal, M. Cortazar, and J. J. Iruin, *J. Appl. Polym. Sci.*, **42**, 489 (1991).
17. J. M. Martinez, J. Nazabal, and J. I. Eguiazabal, *J. Appl. Polym. Sci.*, **51**, 223 (1994).
18. M. Kimura and R. S. Porter, *J. Polym. Sci. Polym. Phys. Ed.*, **22**, 1697 (1984).
19. K. G. Blizzard and D. G. Baird, *Polym. Eng. Sci.*, **27**, 653 (1987).
20. M. K. Nobile, E. Amenderla, and L. Nicolais, *Polym. Eng. Sci.*, **29**, 244 (1988).
21. L. H. Wang, M. Lu, X. Yang, and R. S. Porter, *J. Macromol. Sci. Phys. B*, **29**, 155 (1990).
22. M. F. Cheung, A. Golovoy, R. O. Carter III, and H. Van Oene, *Ind. Eng. Chem. Res.*, **28**, 476 (1989).
23. K. R. Carduner, R. O. Carter III, M. F. Cheung, A. Golovoy, and H. Van Oene, *J. Appl. Polym. Sci.*, **40**, 963 (1990).
24. K. F. Cheung, K. R. Carduner, K. R. Carduner, R. O. Carter III, A. Golovoy, and H. Van Oene, *J. Appl. Polym. Sci.*, **40**, 977 (1990).
25. T. H. Shinn, J. Y. Chen, and C. C. Lin, *J. Appl. Polym. Sci.*, **47**, 1233 (1993).
26. R. W. Lenz, J. I. Jin, and K. A. Feichtinger, *Polymer*, **24**, 327 (1983).
27. V. A. Nicely, J. T. Dougherty, and L. W. Renfro, *Macromolecules*, **20**, 573 (1987).
28. V. L. Gunar, *Macromolecules*, **22**, 3974 (1989).

Received October 27, 1995

Accepted December 20, 1995